Virology 422 (2012) 288–296

Contents lists available at SciVerse ScienceDirect

Virology

journal homepage: www.elsevier.com/locate/yviro

HIV-1 Tat induces biochemical changes in the serum of mice

Wenting Liao [a,b], Guangguo Tan [a], Zhenyu Zhu [a], Qiuli Chen [b], Ziyang Lou [a], Xin Dong [a], Wei Zhang [a], Wei Pan [b,*], Yifeng Chai [a,**]

[a] School of Pharmacy, Second Military Medical University, Shanghai 200433, China
[b] Department of Microbiology, Second Military Medical University, Shanghai 200433, China

ARTICLE INFO

Article history:
Received 19 August 2011
Returned to author for revision
22 September 2011
Accepted 6 November 2011
Available online 21 November 2011

Keywords:
Metabolomics
HIV-1 Tat protein
GC/MS
Multivariate data analysis

ABSTRACT

The HIV-1 Tat protein is released by infected cells and has numerous biological activities which might contribute either to the impairment of the immune response or to viral dissemination and pathogenesis. To date, the effects of Tat protein on metabolites remain unclear. In this study, a metabolomic study on serum of HIV-1 Tat-induced ICR mice was performed to research the pathologic mechanism of Tat protein by using gas chromatography coupled to mass spectrometry (GC/MS). Clear separations among the HIV-1 Tat-induced mice and the inaTat-induced or control mice were observed by principal component analysis and partial least-squares discriminant analysis based on the GC/MS spectral data. Additionally, 16 significantly changed metabolites in HIV-1 Tat-induced mice were identified that are involved in multiple perturbed metabolic pathways, which contributed to the elucidation of the complex pathogenic mechanism of Tat protein and may shed new lights on future improvement of HIV-1 therapy.

Introduction

Human immunodeficiency virus type 1 (HIV-1) Tat is a multifunctional protein that contributes to virus replication as well as several pathological symptoms of HIV-1 infections. Tat is released by infected cells (Chang et al., 1997; Ensoli et al., 1993) and has numerous biological activities that might contribute either to the impairment of the immune response (Cohen et al., 1999; Subramanyam et al., 1993; Viscidi et al., 1989) or to viral dissemination (Huang et al., 1994; Marchio et al., 2005; Smith et al., 2003) and pathogenesis (Barillari and Ensoli, 2002; Ensoli et al., 1990; Sabatier et al., 1991). Tat can affect the expression of many cellular genes, inducing disturbances of signal transduction pathways (Mischiati et al., 1999), angiogenic programs in endothelial cells (Rusnati and Presta, 2002), neuronal apoptosis (Li et al., 2005), and the modulation of the expression of several molecules involved in the initiation of immune responses (Campbell and Loret, 2009). Furthermore, several in vivo experiments have demonstrated detrimental consequences of the presence of Tat in an organism. Studies of transgenic mice expressing Tat suggested that this viral protein may contribute to the growth of many types of tumors that frequently develop in patients during the course of AIDS (Corallini et al., 1993). It has also been shown that Tat stimulates apoptosis in the rat central nervous system and causes neurologic disorders (Gavriil et al., 2000). Furthermore, Tat appears to be immunosuppressive when injected into mice (Agwale et al., 2002; Cohen et al., 1999), and it has also been shown to enhance AZT toxicity in a transgenic mouse model (Prakash et al., 1997). Taken altogether, the pathogenesis of Tat is very complex and needs to be further investigated. Considering its multi-bioactivities, ability to induce a pattern of cytokines and complex pathogenesis, Tat was thought to act as a "viral toxin" (Gallo, 1999). To date, the effects of the Tat protein on metabolites remain unclear.

Metabolomics (the systems biology of small molecules) is a new approach for the untargeted identification of potential biomarkers (Want et al., 2007). Metabolites are obvious candidates for biomarker screening because they represent the downstream effect of enzyme catalysis and other biotransformations, and they are smaller in number than the proteome. Although metabolomics initially emerged using NMR, mass spectrometry (MS) has evolved as a powerful technique for the comprehensive profiling of the metabolome in, for example, serum, urine, and cells (Want et al., 2007). The power of MS in metabolomics arises from its sensitivity, speed, and ability to interface directly with chromatography. Gas chromatography coupled with mass spectrometry (GC/MS) has proven to be a robust metabolomic tool and widely applied in metabolite identification and quantification (Jonsson et al., 2004, 2005) due to its excellent resolution and sensitivity. Coupling bioinformatics and biostatistics with this technology platform permits the identification and quantification of low weight molecules to characterize a whole organism's response to a given condition.

The application of metabolomics to a viral infection or pathogenesis of a viral bioactive protein is a largely unexplored area (Wikoff et al., 2008). Here we present the first GC/MS-based metabolomic study of Tat-induced mice serum. HIV-1 Tat-induced mice were

* Corresponding author.
E-mail addresses: pwpanwei@yahoo.com.cn (W. Pan), yfchai@smmu.edu.cn (Y. Chai).

0042-6822/$ – see front matter © 2011 Elsevier Inc. All rights reserved.
doi:10.1016/j.virol.2011.11.005

characterized by altered levels of serum amino acids, carboxylic acids, fatty acids, and other metabolites, such as lactate, glutamine, uric acid and α-tocopherol, which were related to multiple perturbed metabolic pathways and contributed to the elucidation of the complex pathogenic mechanism of the HIV-1 Tat protein.

Results

Purification and characterization of recombinant Tat protein

The DNA encoding for the HIV-1 HXB2 strain Tat protein was amplified by overlapping PCR and the protein was expressed and purified. The purified Tat protein was relatively pure and free of the bulk of the bacterial proteins as assessed by SDS-PAGE electrophoresis (Fig. 2A, lane 7). Tat is particularly vulnerable to oxidative stresses that modify its structure, inducing protein multimerization and aggregation that leads to the loss of biological activity. Therefore, the purified Tat protein was immediately lyophilized, stored at −80 °C, and then resuspended in degassed PBS just before use.

As shown in Fig. 2A (bottom panel), the recombinant Tat protein was tested and was specifically recognized by an anti-Tat monoclonal antibody by western blot analysis. This finding demonstrated that the protein was successfully expressed and purified.

One serious limitation to recombinant protein expression in *Escherichia coli* is the copurification of lipopolysaccharides (LPS) which is the constituent component of Gram negative bacterial cell walls and could be toxic to the cells and tissues of mammalian origin (Beutler and Rietschel, 2003). Therefore, it is essential to remove endotoxin completely from Tat expressed from a bacterial source. In this study, Triton X-100 at 2% concentration (Petsch and Anspach, 2000; Siddappa et al., 2006) was used to extensively wash the columns to remove endotoxin, which resulted in a reduction of endotoxin levels in the eluted Tat to the order of approximately 500 (reduction from 400 EU/μg to 0.8 EU/μg) and 8000 times (reduction from 400 EU/μg to 0.05 EU/μg) after Ni–NTA and ion-exchange chromatographies, respectively. The final concentration of endotoxin in the eluted Tat was approximately 0.05 EU/μg of protein which is within the acceptable limit (Petsch and Anspach, 2000).

Recombinant Tat protein is transactivation competent

Tat is believed to be secreted into extracellular spaces from infected cells, cross cell and nuclear membranes of the neighboring cells efficiently, and transactivate latent viral promoters, thus enhancing viral infectivity (Ensoli et al., 1993). We tested the ability of the purified recombinant Tat protein to enter target cells and transactivate reporter genes under the control of the viral promoter. 293T cells were transiently transfected with pLTR-GFP and incubated for 24 h. Although the cells transfected with pLTR-GFP and in the absence of Tat showed GFP expression because of the strong constitutive activity of LTR promoter, GFP expression in 293T cells was significantly higher in the presence of Tat (the left panel in Fig. 2B) than that in the presence of PBS (the right panel in Fig. 2B) and inaTat protein (the middle panel in Fig. 2B) suggesting efficient Tat-transactivation by the recombinant Tat protein. In addition, SEAP expression (Fig. 2C) in 293T cells was determined with relative ratio of Tat group (15:1), inaTat (1.8:1), PBS group (1.4:1) to control group (only transfected with the pLTR-GFP), demonstrating that the purified Tat protein is bioactive.

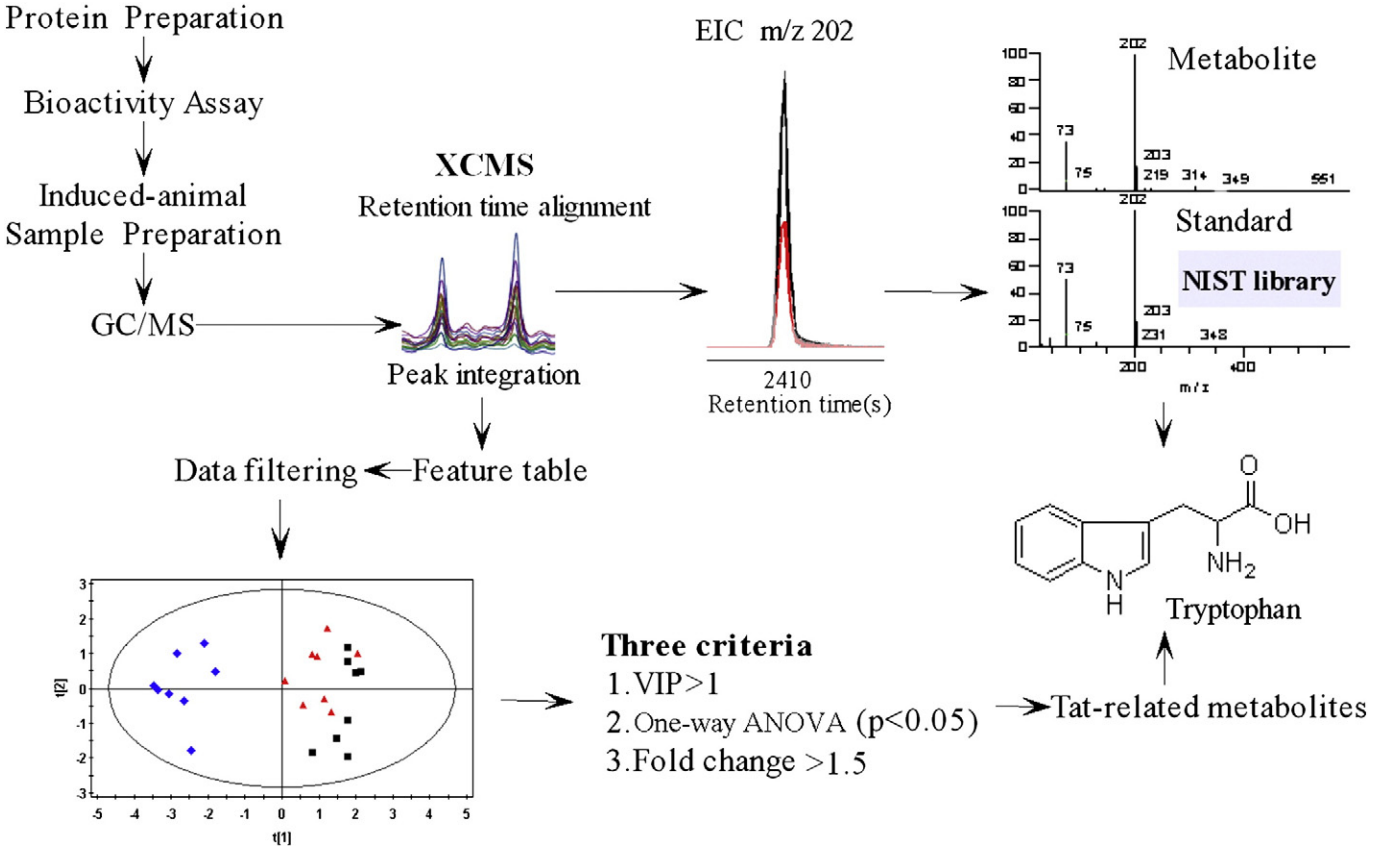

Fig. 1. Schematic flowchart of the metabolic profiling strategy used in this study. The recombinant Tat protein was expressed and purified, and its bioactivity was evaluated. ICR mice were treated with the bioactive Tat protein, inaTat or PBS. Serum samples were extracted, derivatized and subsequently analyzed by GC/MS. Multivariate statistics was applied to extract meaningful information in the complex GC/MS spectral data. Compounds with significant contribution to the variation of metabolic profiles among the HIV-1 Tat-induced samples and the inaTat-induced or control samples were identified using GC/MS NIST library and further verified by reference compounds available.

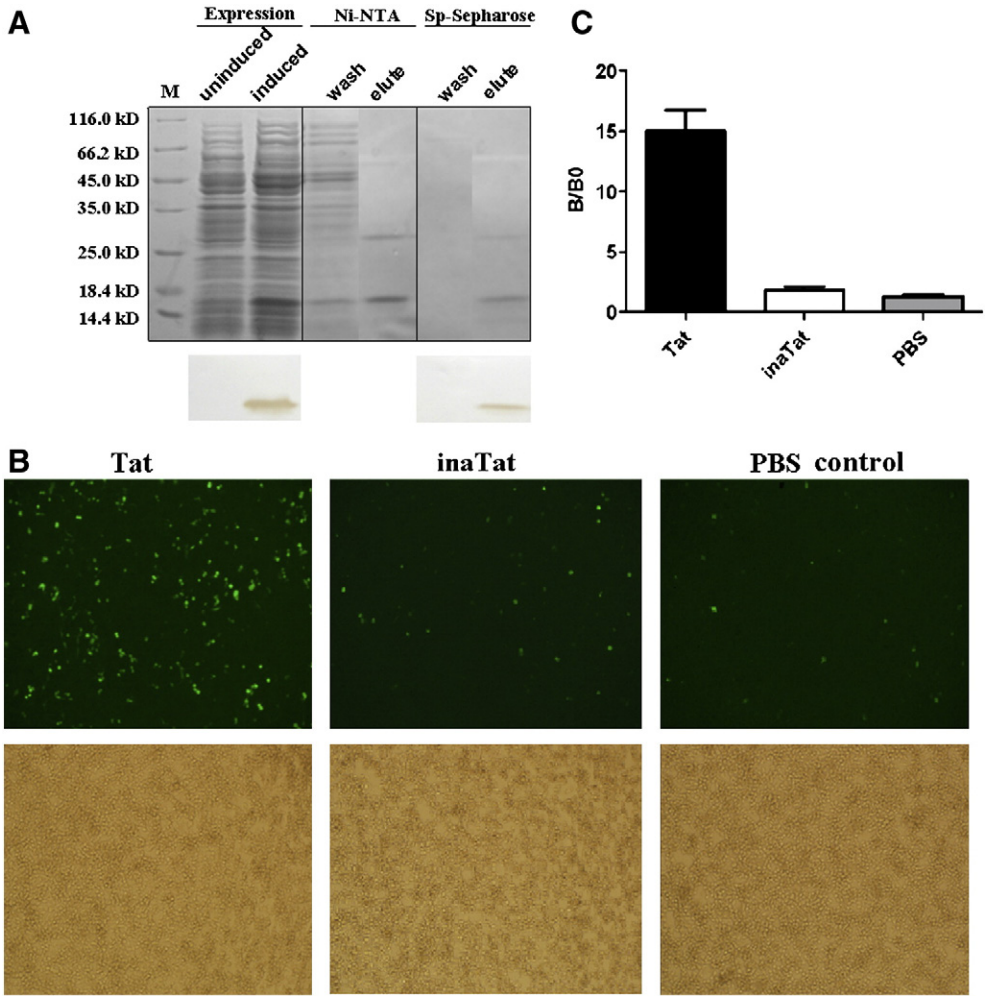

Fig. 2. (A) SDS-PAGE and western blot analyses of the purified Tat protein. The Tat protein was expressed and purified by Ni–NTA affinity chromatography and further purified by SP Sepharose fast flow ion-exchange chromatography. A measured quantity of the protein was resolved on a 15% SDS-PAGE gel with protein molecular weight standards (M; Sigma, St. Louis, Mo). Bottom panel shows the western blot analysis of the Tat protein resolved on a duplicate SDS-PAGE and electrophoretically transferred to a PVDF membrane. An anti-Tat monoclonal antibody was used for the western blot analysis. (B) The recombinant Tat protein is transactivation competent. 293T cells were transiently transfected with pLTR-GFP using a commercial lipid formulation. Twenty-four hours after the transfection, the cells were incubated with bioactive Tat protein, inaTat or PBS. Twenty-four hours following the protein transfection, expression of GFP was measured using UV-fluorescence microscopy. The top group was fluorescent view and the bottom group was fluorescent view with corresponding light view. (C) Expression of alkaline phosphatase secreted into the medium was estimated at 24 h using lumino-meter. B, chemiluminescence values measured using lumino-meter; B_0, background SEAP expressed by 293T without Tat.

Analysis of Tat-induced metabolites by untargeted metabolomics

The stability of the analytical method is very important to obtain valid metabolomic data. In this study, the system stability was expressed as the relative standard deviation (RSD) of the relative peak areas of eight common ions (see section "System stability"). The result was 6.17%–12.56%, demonstrating the robustness of the method. This finding means that differences amid the test samples from different individuals were more likely to reflect varied metabolite profiles rather than analytical variation.

The typical total ion current chromatograms (TICs) of mouse sera are shown in Fig. 3. By untargeted filtration of ion peaks, the data were simplified and 214 ion peaks were obtained. Application of PCA to the data differentiated the control, inaTat and Tat-induced groups ($R^2 = 0.52$). As shown in Fig. 4A, all the samples of Tat group are distributed in the left side of the figure and are well separated from those of control and inaTat groups. Conversely, all of the samples from control and inaTat groups are distributed in the right side of the figure and the inaTat group was close to the control group. It suggested that inaTat protein caused the similar changes to PBS control. The supervised approach of PLS-DA was more focused on the actual class discriminating variation in the data compared to the unsupervised approach of PCA. A clear separation among the Tat-induced group and the inaTat or control group was observed in the PLS-DA score plot by the first two components (Fig. 4B) ($R^2 = 0.89$, $Q^2 = 0.81$). To validate the model, permutation tests with 100 iterations were further performed. These permutation tests compared the goodness of fit of the original model with the goodness of fit of randomly permuted models. As shown in Fig. 4C, the validation plot indicates that the original model is valid. The criteria for validity are as follows: all the permuted R^2 (cum) and Q^2 (cum) values to the left are lower than the original point to the right, and the blue regression line of the Q^2 (cum) points has a negative intercept (Mahadevan et al., 2008; Pasikanti et al., 2010).

Among the 214 metabolites detected, 98 metabolites were identified from serum samples that differed statistically significant between the groups after correction for multiple comparisons (false discovery rate $Q<0.05$). Variables that significantly contributed to the clustering and discrimination were identified according to a threshold of variable importance in the projection (VIP) values (VIP >1), which could be generated after PLS-DA processing. According to the VIP value, the 30 variables were selected as the candidates of potential biomarkers. Some of these variables were found to be from the same metabolites. After merging the variables from the identical

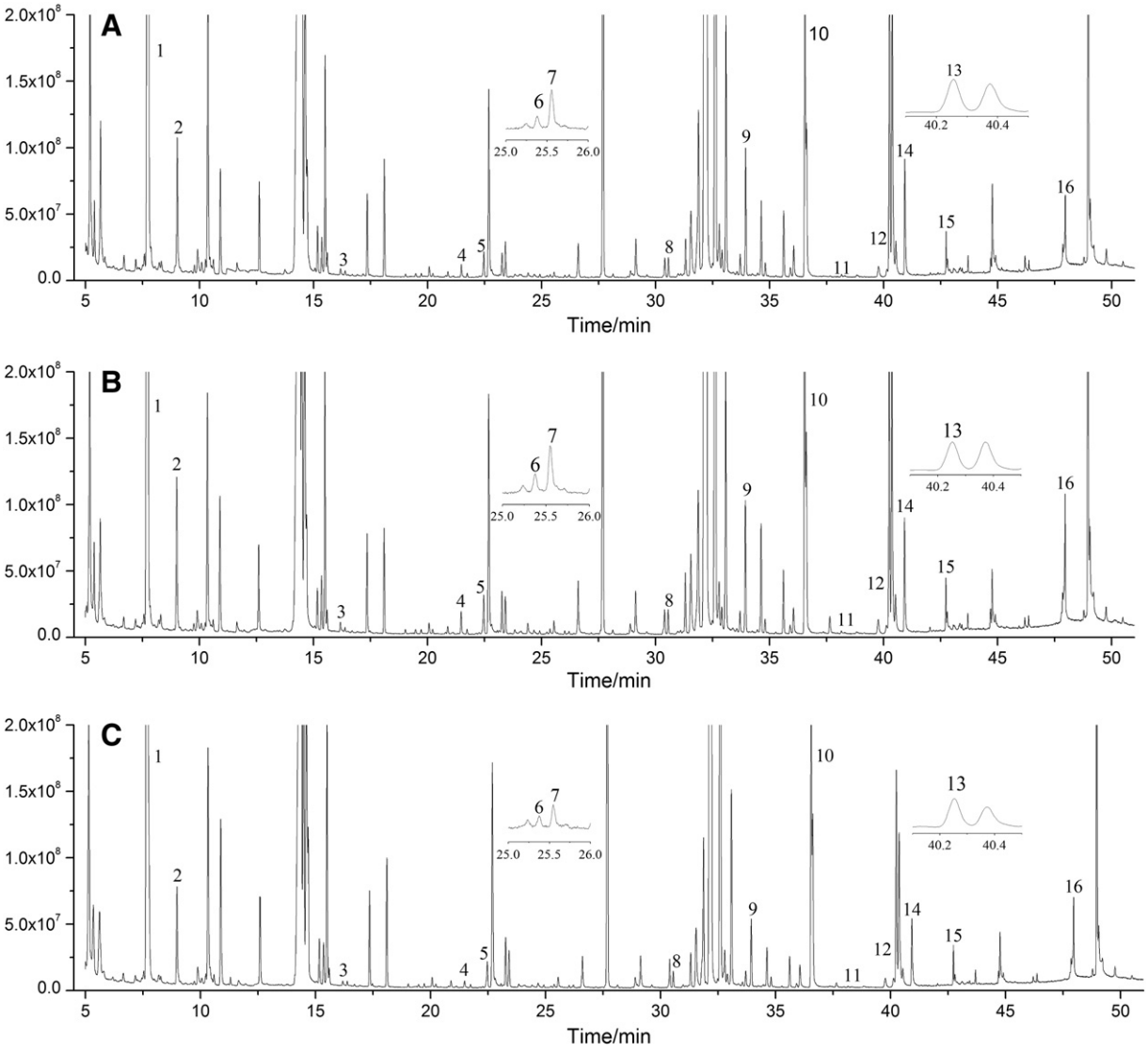

Fig. 3. The typical total ion current chromatograms (TICs) of mouse sera from the control group (A), the inaTat group (B) and the Tat group (C).

metabolites, 22 variables were collected. Moreover, the criteria were further restricted to features with an average intensity difference of at least 1.5-fold (high or low) between inaTat- and Tat-induced samples. Following the criterion above, 16 significantly differential variables were found, which were considered as potential biomarkers. The results are listed in Table 1.

Discussion

The complex pathogenesis of HIV-1 Tat is still a challenging field and an effective in vivo model is necessary. To date, several Tat-transgenic mice models have been successfully created to study HIV-1 Tat-induced pathology (Giunta et al., 2009; Kim et al., 2003; Prakash et al., 1997). Recently, Atrayee Banerjee et al. reported an ICR mouse model injected intravenously with bioactive Tat protein was used to study oxidative stress-induced damage in the brain and potential role of antioxidant (Banerjee et al., 2010). In this study, the similar ICR mouse model combined with GC/MS-based metabolomic profiling approach was applied to investigate whether this system could identify signatures associated with pathogenesis of the Tat protein in Tat-treated mice serum. The GC/MS-based metabolic profiling platform combined with multivariate statistical methods (PCA and PLS-DA) has enabled us to highlight the organism's distinct response to Tat, and 16 metabolites were identified with statistically significant changes in Tat-induced mice, which are discussed as follows.

Tryptophan was significantly decreased in the serum of Tat-induced mice. As essential amino acid, tryptophan uptake in the diet may lead to the same result. We treated the mice for 5 days with Tat protein, and observed that this treatment did not change the animal diet behavior and cause weight loss. Therefore, it can be presumed that the decrease of tryptophan in this study has been probably attributed to increased tryptophan metabolism. Consistent with our result, significantly decreased blood levels of the essential amino acid tryptophan in infected individuals were noted fairly early on in the HIV epidemic (Larsson et al., 1989; Werner et al., 1988). Confirming those early reports, a 2003 survey of the data from 16 published studies suggested that, despite adequate dietary intake, the average tryptophan blood level in HIV infected individuals is almost 30% below that of normal uninfected individuals (Murray, 2003). The reduction of tryptophan could be due to two factors. On the one hand, tryptophan can enter the brain where it is degraded by the kynurenine pathway (Ruddick et al., 2006). On the other hand, tryptophan may also be degraded in various cells as Tat was found to up-regulate indoleamine-2,3-dioxygenase (IDO), the rate-limiting enzyme of tryptophan metabolism, and

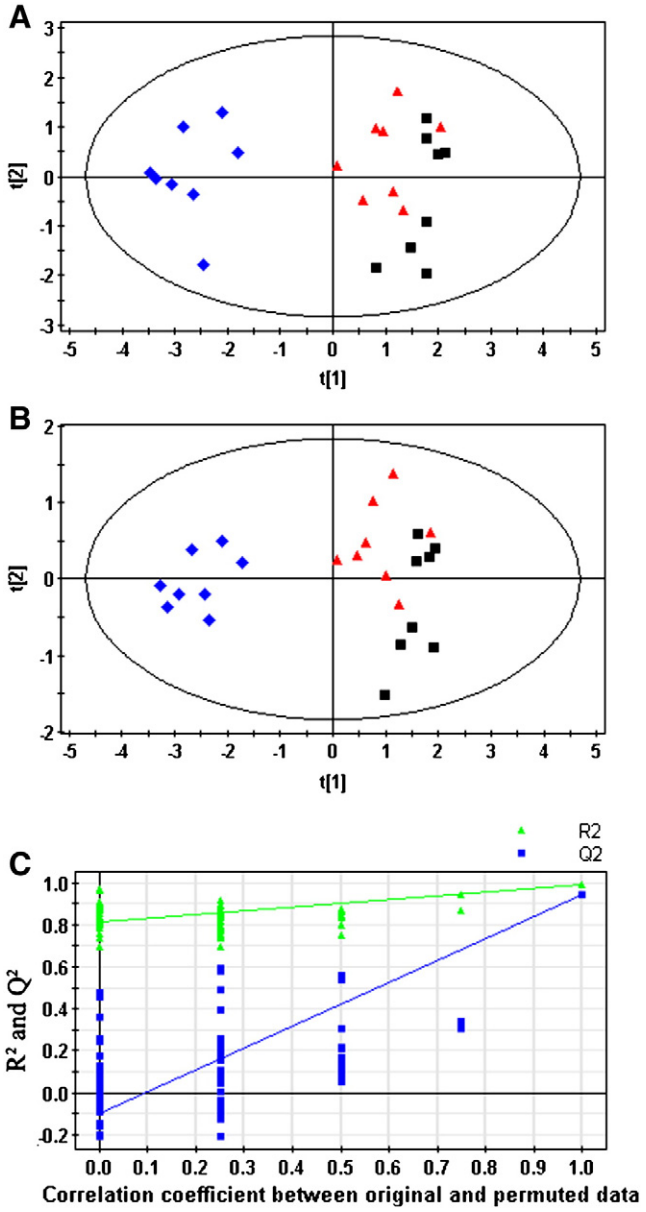

Fig. 4. (A) PCA score map derived from GC/MS spectra concerning control (■), inaTat (▲) and Tat (♦) samples. (B) PLS-DA score map derived from GC/MS spectra concerning control (■), inaTat (▲) and Tat (♦) samples. (C) Validation plot obtained from 100 permutation tests.

down-regulate 5-HTT expression in immature dendritic cells (Samikkannu et al., 2010). This Tat-induced abnormal tryptophan metabolism could be associated with its pathogenesis, which will be further evaluated.

Lactate, a potential source of endogenous molecular toxins, is the end product of glycolysis. Jiang et al. reported that increased lactate is a key biomarker related to lipodystrophy (Jiang et al., 2008), which often occurs in HIV-infected patients (Sekhar et al., 2002). Lipodystrophy has not only been strongly associated with antiretroviral treatments, but it may be associated with the viral infection itself (Slama et al., 2009). Recent studies indicate that some viral proteins may impede adipocyte differentiation by decreasing peroxisome proliferator-activated receptor-gamma (PPARγ) expression and contribute to lipodystrophy (Shrivastav et al., 2008). Higher levels of lactate were observed in the Tat-induced mice compared to inaTat and control group in our study and we infer that the increased lactate level induced by the HIV-1 Tat protein may also contribute to HIV-associated lipodystrophy.

Palmitinic acid and stearic acid were present in decreased levels in the Tat-induced group, which suggested that Tat protein may inhibit fatty acids synthesis or enhance β-oxidation of fatty acids. Arachidonic acid, a polyunsatured fatty acid, serving as a biologically active signaling molecule as well as an important component of membrane lipid, exerts many biological functions including modulation of the activities of protein kinases and ion channels (Khan et al., 1995). Jiang et al. provided evidence that HIV Tat promoted arachidonic acid metabolism which contributed to HIV-1 Tat-mediated transactivation, and drugs that anti-arachidonic acid properties may be responsible for their HIV-Tat inhibitory capability (Jiang et al., 1996). In this study, arachidonic acid was proved again to be decreased in Tat-treated mice, which suggested a possible link of arachidonic acid pathway to bioactivity of HIV-1 Tat protein.

The citrate cycle is central to aerobic metabolism, facilitating adequate throughout of substrates derived from carbohydrates, fatty acids or certain amino acids (Sabatine et al., 2005). As pivotal intermediates of TCA cycle, the decreased levels of citrate, succinate and malate in the Tat-induced group indicated that TCA cycle was inhibited. This phenomenon may be attributed to the decreased activity of citrate synthase in mitochondria, where TCA metabolism occurs (Prasada Rao and Gardner, 1986). In addition, Tat was previously reported to induce oxidative stress (Pocernich et al., 2005), and under the circumstance, TCA cycle slows during cellular regulation to reduce the natural production of ROS (Huang et al., 2008). Thus, we infer that the decreased levels of citrate, succinate and malate are due to the dysfunction of mitochondria, and the block of natural energy production by Tat-induced oxidative stress. In addition, α-amino acids are critical to life and have a variety of roles in metabolism. They are not only the building blocks of proteins and coenzymes but are also important energy metabolism materials and can be transformed into some metabolism intermediates such as pyruvate, oxaloacetic acid, oxoglutarate, citric acid and fumarate, to participate in the tricarboxylic acid (TCA) cycle. In the Tat-induced group, four amino acids (L-alanine, proline, phenylalanine and tyrosine) were decreased in circulation. One possible speculation was that oxidative stress caused by Tat protein lead to the metabolic remodeling of α-amino acids to meet energy requirement.

GC/MS analysis showed significantly decreased levels of glutamine in the serum of the Tat-induced mice. Glutamine is the main precursor of the excitatory neurotransmitter glutamate. This glutamine/glutamate cycle is essential for glutamine homeostasis and neurotransmitter glutamate generation and recycling (Schousboe, 2003). Glutamate induced neurotoxicity has been implicated in HIV-associated dementia (Silvers et al., 2007), and the toxic effects are closely related to the HIV Tat protein, which is involved in glutamatergic effects (Holden et al., 1999; Perez et al., 2001). Decreased serum glutamine may contribute to glutamate induced neurotoxicity (Ramonet et al., 2004).

Uric acid, which is involved in purine metabolism, was significantly decreased in the Tat-induced mice. Purine metabolism had been studied in peripheral blood lymphocytes (PBL) of normal subjects and HIV-l infected patients (Carlucci et al., 1996; Tabucchi et al., 1992, 1993). It was found that viral penetration affected purine nucleotide metabolism of total PBL. Nucleosides and nucleobases, which are catabolic products, were significantly lower. In this study, uric acid as catabolic products of purine metabolism was also decreased in the Tat-induced mice. While we failed to detect other metabolites in purine metabolism pathway, we cannot clearly delineate this impact on purine metabolism. In addition, uric acid is an important non-enzymatic antioxidant. The decreased levels of serum uric acid indicated a defect in the antioxidant defense, which played an important role in oxidative stress in HIV-associated dementia (Pocernich et al., 2005).

Table 1
Potential biomarkers in Tat-induced mice serum.

Peak no.	Identity	Retention time (min)	P value[a]	Fold change[b]	Control group mean (S.D.)[c]	inaTat group mean (S.D.)[d]	Tat group mean (S.D.)[e]
1	Lactate	7.72	<0.0001	0.64	6.0295 (0.4657)	6.1706 (0.4742)	9.6169 (0.5214)
2	L-alanine	9.00	0.0006	1.50	0.4806 (0.0753)	0.4754 (0.0788)	0.3178 (0.0549)
3	Succinate	16.19	<0.0001	1.61	0.0041 (0.0007)	0.0040 (0.0005)	0.0025 (0.0003)
4	Malate	21.48	0.0031	1.59	0.0077 (0.0014)	0.0068 (0.0017)	0.0043 (0.0006)
5	Proline	22.47	0.0004	1.97	0.0418 (0.0077)	0.0361 (0.0069)	0.0184 (0.0039)
6	Glutamine	25.38	0.0002	1.83	0.0156 (0.0031)	0.0135 (0.0027)	0.0074 (0.0014)
7	Phenylalanine	25.55	0.0001	1.85	0.0406 (0.0076)	0.0352 (0.0029)	0.0190 (0.0032)
8	Citrate	30.56	0.0010	1.59	0.0264 (0.0046)	0.0266 (0.0048)	0.0167 (0.0039)
9	Tyrosine	33.71	0.0032	1.70	0.0048 (0.0009)	0.0042 (0.0009)	0.0025 (0.0010)
10	Palmitinic acid	36.55	<0.0001	1.53	0.5553 (0.0398)	0.5210 (0.1052)	0.3416 (0.0698)
11	Uric acid	37.66	<0.0001	5.59	0.0146 (0.0018)	0.0139 (0.0026)	0.0025 (0.0005)
12	Tryptophan	40.17	0.0002	1.51	0.0100 (0.0012)	0.0084 (0.0013)	0.0055 (0.0008)
13	Linoleic acid	40.25	<0.0001	1.61	0.1625 (0.0101)	0.1593 (0.0142)	0.0988 (0.0153)
14	Stearic acid	40.93	0.0003	1.55	0.1102 (0.0104)	0.1061 (0.0219)	0.0683 (0.0121)
15	Arachidonic acid	42.81	0.0002	1.61	0.0035 (0.0005)	0.0034 (0.0006)	0.0021 (0.0004)
16	α-Tocopherol	48.78	0.0005	1.51	0.0115 (0.0013)	0.0113 (0.0023)	0.0075 (0.0012)

[a] Tat group versus inaTat group.
[b] The fold change of relative amounts of the inaTat group compared to the Tat group.
[c] The ratio of peak area to the internal standard on the same chromatogram from the control group; the data were represented as the mean (S.D.).
[d] The ratio of peak area to the internal standard on the same chromatogram from the inaTat group.
[e] The ratio of peak area to the internal standard on the same chromatogram from the Tat group.

α-Tocopherol was significantly decreased in the Tat-induced mice, which was consistent with the variation tendency of α-tocopherol levels in the plasma samples of monkeys with SIVE (Pendyala et al., 2010). α-Tocopherol is an important compound of vitamin E, which is comprised of eight related tocopherols and tocotrienols, and maintains physiological cellular and tissue functions through the antioxidant properties of these compounds. The decreased levels of α-tocopherol may contribute to oxidation stress damage induced by the HIV Tat protein (Pocernich et al., 2005).

Based on our findings, an integrative view plot of the metabolite change induced by Tat protein in the circulation system is shown in Fig. 5. In conclusion, this is the first metabolomic study to determine the biochemical alterations in the serum of HIV-1 Tat-induced mice by using GC/MS. We identified 16 significantly changed metabolites involved in amino acid metabolism, glycolysis, TCA cycle and fatty acid metabolism, which were helpful for revealing the complex pathogenic mechanism of HIV-1 Tat as a viral toxin and may shed new light on future improvements of HIV-1 therapy.

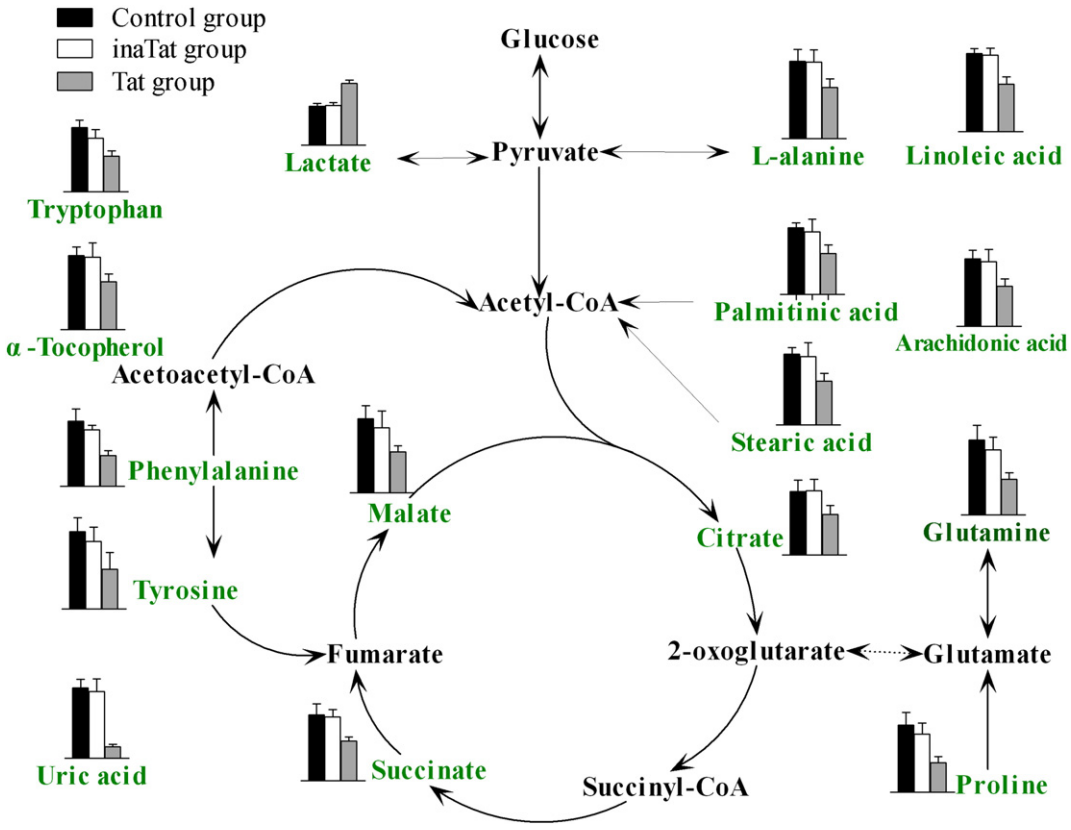

Fig. 5. The integrative view plot of the metabolite change induced by the Tat protein in the circulation system. Column value in histograms is expressed as mean ± S.D., in which the values are the relative peak area ratios of the 16 metabolites to ribitol.

Metabolomic analysis

Sample collection and preparation

All mice were sacrificed 6 days after the treatment, and sera were collected into standard vials from the retro-orbital venous sinus. Blood samples were allowed to clot at room temperature for 30 min, and then the serum was separated by centrifugation at 3000 ×*g* for 10 min at 4 °C and stored at −70 °C until the analysis.

Before the analysis, serum (100 μl) was transferred into a centrifuge tube and spiked with the internal standard (5 μl of 1 mg/ml of ribitol), followed by adding 400 μl of methanol/acetonitrile/acetone (1:1:1, v/v/v) (Bruce et al., 2009) into the tube. After vigorous shaking for 1 min and incubation on ice for 10 min, the mixture was centrifuged at 14,000 ×*g* for 15 min at 4 °C to precipitate the protein. The supernatant (200 μl) was transferred into a GC vial and dried with a gentle nitrogen stream. The derivatization was performed using methoxyamine pyridine (75 μl; 15 mg/ml) at 70 °C for 1 h, followed by MSTFA (75 μl) with 1% TMCS as catalyst at room temperature for 1 h. n-Heptane (200 μl) was added to dilute the solution after the derivatization, and the supernatant was used for GC/MS analysis.

GC/MS analysis

The derivatized samples for GC/MS were analyzed on a Thermo-Finnigan Trace DSQ fasting scanning single-quadrupole MS (Thermo Electron Corporation) operated at unit mass resolving power. A 0.5 μl of sample solution was injected with splitless mode to a TR-5MS column (30 m × 250 μm × 0.25 μm) with helium as the carrier gas at a flow of 1 ml/min. The injector temperature was set at 260 °C. The temperature of the ion source was adjusted to 200 °C and that of the quadrupole was set at 150 °C. GC/MS was operated using electron impact ionization with a 60–600 amu scan range. The initial temperature of the column was kept at 70 °C for 3 min. Then, the temperature was ramped at 4 °C/min to 220 °C and then to 310 °C at a rate of 12 °C/min where it was held for 10 min. To reduce systematic error associated with instrument drift, samples were run in an order that alternated between the Tat-induced group and the control group. Each sample was run in duplicate, and after data integration, duplicate runs were averaged.

We first searched the NIST database installed in the Thermo-Finnigan Trace DSQ GC/MS system for the identification of the metabolites based on the GC/MS data. Candidate compounds showing higher similarities (>75%) were selected. Lastly, the exact identities of the metabolites of interest were verified by commercial standards.

System stability

To evaluate the applicability of the GC/MS method, an equal volume of each sample was pooled together to construct an artificial sample. This sample was processed as a real sample, and then it was randomly inserted in the real sample queue to be analyzed six times accordingly. The system stability was expressed as the relative standard deviation (RSD) of the relative peak areas, i.e., the ratios of the peak areas of the metabolites to that of the internal standard. Eight common extracted ion chromatograms (EICs) shared by these injections were selected based on their relatively high abundance levels and wide retention time distribution range in the chromatogram.

Data analysis

Data in an instrument-specific format were converted to CDF format files. The program XCMS was used for nonlinear alignment of the data in the time domain and automatic integration and extraction of the peak intensities. XCMS parameters were default settings except for the following: fwhm = 4, bw = 5 and snthersh = 5. The output data were imported into MATLAB 7.0 software (The MathWorks, Inc., USA), where data were normalized using the summation of response of all metabolites in one sample and then calculated the ratios of the intensities of mass ions to that of the internal standard fragment ion (m/z 216.9, it is the most abundance fragment ion for the silylation derivative of ribitol).

It should be noted that GC/MS data inherently contain apparent variability and complexity, such as multiple fragment ions from a single compound. Directly concatenating the matrices of processed-MS data is suboptimal as this may result in a matrix with an unfavorable samples-to-variables ratio. It is necessary to use a properly reduced matrix to conduct multivariate statistical analysis. A simple strategy was untargeted filtration of ion peaks using our in-house scripts in the MATLAB 7.0, where the most abundant fragment ion with the same retention time (the time bin is 0.01 min) remained and the other ions were excluded.

The processed data list was exported and processed by the principal component analysis (PCA) and partial least-squares discriminant analysis (PLS-DA) in SIMCA-P software (Version 11, Umetrics). It should be noted that data were log transformed for multivariate analysis to eliminate the unit error. The significance was expressed by using one-way ANOVA analysis of the SPSS 13.0 for Windows (SPSS Inc., Chicago, IL, USA). P-values less than 0.05 were considered significant. Significant peak changes between samples were confirmed by manual quantification by calculating the area under the peak from raw chromatograms. To account for multiple comparisons, false discovery rate was estimated as the maximum Q value (Storey, 2002) in the set of significant differences for the metabolomic data set. False discovery rates were computed using the R package Q value. The significance of the group differences was evaluated by the P value for the fixed-effect parameter estimate of group differences.

Materials and methods

The schematic flowchart of the metabolic profiling strategy used in this study is illustrated in Fig. 1.

Reagents

Methoxylamine hydrochloride, N-methyl-N-(trimethylsilyl)-trifluoracetamide (MSTFA), pyridine, trimethyl-chlorosilane (TMCS), n-heptane, acetone, and citrate were purchased from Sigma-Aldrich (St. Louis, MO, USA). Methanol and acetonitrile are chromatography pure (Merck, Germany). The following compounds were obtained from Shanghai Jingchun Reagent Co.: ribitol, lactate, L-alanine, sodium succinate, malic acid, L-proline, L-glutamine, phenylalanine, tyrosine, palmitinic acid, stearic acid, linoleic acid and arachidonic acid.

Preparation of recombinant Tat protein

The DNA encoding for Tat protein (1–86 aa) from the BH-10 clone of the IIIB strain of HIV-1 (clade B) was amplified by overlapping PCR and cloned into the NdeI and XhoI site of the bacterial expression vector pET21b (Novagen) under the control of the T7 promoter. We added a His-tag of 6 amino acid residues to the C-terminus of Tat to facilitate purification via Ni–NTA chromatography, and we expressed the protein in *E. coli.* The Tat protein was then purified as previously described (Siddappa et al., 2006). Briefly, individual bacterial colonies (*E. coli* BL21 (DE3)) were grown in 1 l cultures in LB medium supplemented with 100 μg/ml ampicillin. Protein production was induced by adding IPTG at final concentration of 1 mM to the cultures when they reached an OD of 0.4, and we incubated the cultures for an additional 3 h at 37 °C. The protein was identified in its soluble form. Cells were harvested by high-speed centrifugation and resuspended in 20 ml of lysis buffer. The bacteria were lysed by sonication and then centrifuged at 14,000 ×*g* for 30 min at 4 °C to remove cell debris.

The protein was obtained from the supernatant, purified by affinity chromatography (a Ni–NTA column (QIAGEN)), and then further purified by SP Sepharose fast flow ion-exchange chromatography (Amersham Biosciences) following the manufacturer's instructions. The lyophilized Tat protein was resuspended in degassed PBS just before use. Tat protein was heat-inactivated by incubation at 85 °C for 30 min as previously described (Avraham et al., 2004). The heat-inactivated Tat protein (inaTat) has been extensively used as a negative control for bioactive Tat (Avraham et al., 2004; Chi et al., 2011; Perry et al., 2010) and was used as a control for the Tat-induced biochemical changes in this study.

Endotoxin level of purified recombinant Tat protein was determined using the Limulus amebocyte lysate test (BioWhittaker, Inc.).

Western blot analysis of the recombinant Tat protein

The recombinant Tat protein was boiled for 5 min in gel loading buffer, resolved on a 15% SDS-PAGE gel, and then transferred to a polyvinylidene difluoride (PVDF) membrane (Pharmacia). The membrane was blocked with 3% BSA and probed with an anti-Tat monoclonal antibody (NIH AIDS Reagent Repository), diluted at 1:1000 in PBS, at room temperature for 2 h. Membranes were washed and incubated with a secondary antibody conjugated to horseradish peroxidase (Sigma, St. Louis, Mo). The blot was developed by incubating the membrane in the substrate solution containing 3 μl/ml H_2O_2 and 0.5 mg/ml 3,3′-diaminobenzidine tetrahydrochloride (Sigma, St. Louis, Mo) in PBS.

Identification of bioactivity of the recombinant Tat protein

Human embryonic kidney (HEK) 293T cells (purchased from the Cell Bank of Shanghai Institutes for Biological Sciences, Chinese Academy of Sciences, Shanghai, China) seeded in 96-well plates were transiently transfected with 0.5 μg of a plasmid vector encoding green fluorescent protein (GFP) and secreted alkaline phosphatase (SEAP) under the control of the subtype-B LTR (B-LTR) (pLTR-GFP, provided by Dr. Udaykumar Ranga) using a commercial lipid formulation following the manufacturer's directions (Invitrogen). Twenty-four hours after the transfection, the cells were incubated with bioactive Tat protein or inaTat at a final concentration of 5 μg/ml in complete medium. Twenty-four hours following the protein transfection, expression of GFP was measured using UV-fluorescence microscopy. Expression of alkaline phosphatase secreted into the medium was estimated at 24 h using lumino-meter (Toyobo). Cells transfected with the pLTR-GFP plasmid were included as a negative control.

Animal experiments

Twenty-four male ICR mice, 8 weeks of age and weighing approximately 30 g, were provided by the Experimental Animal Center of the Second Military Medical University (Shanghai, China). The colony room was maintained at proper temperature and humidity and was on a 12 h light/dark cycle. The animals had unlimited access to rodent chow and water, and they were used after 1 week of acclimatization. Twenty-four male ICR mice were randomly divided into three groups ($n=8$): Tat group (100 ng in PBS, i.v.), inaTat group (100 ng in PBS, i.v.) and control group (PBS, i.v.). The mice were administered Tat, inaTat, or PBS for 5 consecutive days as previously described (Banerjee et al., 2010).

Acknowledgments

We thank Dr. Udaykumar Ranga (Jawaharlal Nehru Centre for Advanced Scientific Research (JNCASR), Jakkur, Bangalore, India) for generously providing the pLTR-GFP plasmid. This work was funded by the National Natural Science Foundation of China (NSFC) [grant numbers 30972632 and 30872405], the Shanghai Committee of Science and Technology [08JC1405200], the Chinese National Key Special Project for the Prevention and Control of Major Infectious Diseases [2009ZX10004-105], and the Chinese National Key Special Project for Major New Drug Discovery [2011ZX09506-001].

References

Agwale, S.M., Shata, M.T., Reitz, M.S., Kalyanaraman, V.S., Gallo, R.C., Popovic, M., Hone, D.M., 2002. A Tat subunit vaccine confers protective immunity against the immune-modulating activity of the human immunodeficiency virus type-1 Tat protein in mice. Proc. Natl. Acad. Sci. U. S. A. 99 (15), 10037–10041.

Avraham, H.K., Jiang, S., Lee, T.H., Prakash, O., Avraham, S., 2004. HIV-1 Tat-mediated effects on focal adhesion assembly and permeability in brain microvascular endothelial cells. J. Immunol. 173 (10), 6228–6233.

Banerjee, A., Zhang, X.S., Manda, K.R., Banks, W.A., Ercal, N., 2010. HIV proteins (gp120 and Tat) and methamphetamine in oxidative stress-induced damage in the brain: potential role of the thiol antioxidant N-acetylcysteine amide. Free Radic. Biol. Med. 48 (10), 1388–1398.

Barillari, G., Ensoli, B., 2002. Angiogenic effects of extracellular human immunodeficiency virus type 1 Tat protein and its role in the pathogenesis of AIDS-associated Kaposi's sarcoma. Clin. Microbiol. Rev. 15 (2), 310–326.

Beutler, B., Rietschel, E.T., 2003. Innate immune sensing and its roots: the story of endotoxin. Nat. Rev. Immunol. 3 (2), 169–176.

Bruce, S.J., Tavazzi, I., Parisod, V., Rezzi, S., Kochhar, S., Guy, P.A., 2009. Investigation of human blood plasma sample preparation for performing metabolomics using ultrahigh performance liquid chromatography/mass spectrometry. Anal. Chem. 81 (9), 3285–3296.

Campbell, G.R., Loret, E.P., 2009. What does the structure-function relationship of the HIV-1 Tat protein teach us about developing an AIDS vaccine? Retrovirology 6, 50.

Carlucci, F., Tabucchi, A., Perrett, D., Pizzichini, M., Rosi, F., Pagani, R., Marinello, E., 1996. Purine metabolism in HIV-1 virus-infected T lymphocyte population. Biomed. Pharmacother. 50 (10), 505–509.

Chang, H.C., Samaniego, F., Nair, B.C., Buonaguro, L., Ensoli, B., 1997. HIV-1 Tat protein exits from cells via a leaderless secretory pathway and binds to extracellular matrix-associated heparan sulfate proteoglycans through its basic region. AIDS 11 (12), 1421–1431.

Chi, X., Amet, T., Byrd, D., Chang, K.-H., Shah, K., Hu, N., Grantham, A., Hu, S., Duan, J., Tao, F., Nicol, G., Yu, Q., 2011. Direct effects of HIV-1 Tat on excitability and survival of primary dorsal root ganglion neurons: possible contribution to HIV-1-associated pain. PLoS One 6 (9), e24412.

Cohen, S.S., Li, C., Ding, L.N., Cao, Y.Z., Pardee, A.B., Shevach, E.M., Cohen, D.I., 1999. Pronounced acute immunosuppression in vivo mediated by HIV Tat challenge. Proc. Natl. Acad. Sci. U. S. A. 96 (19), 10842–10847.

Corallini, A., Altavilla, G., Pozzi, L., Bignozzi, F., Negrini, M., Rimessi, P., Gualandi, F., Barbantibrodano, G., 1993. Systemic expression of Hiv-1 Tat gene in transgenic mice induces endothelial proliferation and tumors of different histotypes. Cancer Res. 53 (22), 5569–5575.

Ensoli, B., Barillari, G., Salahuddin, S.Z., Gallo, R.C., Wong-Staal, F., 1990. Tat protein of HIV-1 stimulates growth of cells derived from Kaposi's sarcoma lesions of AIDS patients. Nature 345 (6270), 84–86.

Ensoli, B., Buonaguro, L., Barillari, G., Fiorelli, V., Gendelman, R., Morgan, R.A., Wingfield, P., Gallo, R.C., 1993. Release, uptake, and effects of extracellular human immunodeficiency virus type 1 Tat protein on cell growth and viral transactivation. J. Virol. 67 (1), 277–287.

Gallo, R.C., 1999. Tat as one key to HIV-induced immune pathogenesis and Pat toroid as an important component of a vaccine. Proc. Natl. Acad. Sci. U. S. A. 96 (15), 8324–8326.

Gavriil, E.S., Cooney, R., Weeks, B.S., 2000. Tat mediates apoptosis in vivo in the rat central nervous system. Biochem. Biophys. Res. Commun. 267 (1), 252–256.

Giunta, B., Hou, H., Zhu, Y., Rrapo, E., Tian, J., Takashi, M., Commins, D., Singer, E., He, J., Fernandez, F., Tan, J., 2009. HIV-1 Tat contributes to Alzheimer's disease-like pathology in PSAPP mice. Int. J. Clin. Exp. Pathol. 2 (5), 433–443.

Holden, C.P., Haughey, N.J., Nath, A., Geiger, J.D., 1999. Role of Na+/H+ exchangers, excitatory amino acid receptors and voltage-operated Ca2+ channels in human immunodeficiency virus type 1 gp120-mediated increases in intracellular Ca2+ in human neurons and astrocytes. Neuroscience 91 (4), 1369–1378.

Huang, L.M., Joshi, A., Willey, R., Orenstein, J., Jeang, K.T., 1994. Human immunodeficiency viruses regulated by alternative trans-activators: genetic evidence for a novel non-transcriptional function of Tat in virion infectivity. EMBO J. 13 (12), 2886–2896.

Huang, X., Shao, L., Gong, Y., Mao, Y., Liu, C., Qu, H., Cheng, Y., 2008. A metabonomic characterization of CCl4-induced acute liver failure using partial least square regression based on the GC/MS metabolic profiles of plasma in mice. J. Chromatogr. B Analyt. Technol. Biomed. Life Sci. 870 (2), 178–185.

Jiang, M.-C., Lin, J.-K., Chen, S.S.L., 1996. Inhibition of HIV-1 Tat-mediated Transactivation by quinacrine and chloroquine. Biochem. Biophys. Res. Commun. 226 (1), 1–7.

Jiang, N., Yan, X., Zhou, W., Zhang, Q., Chen, H., Zhang, Y., Zhang, X., 2008. NMR-based metabonomic investigations into the metabolic profile of the senescence-accelerated mouse. J. Proteome. Res. 7 (9), 3678–3686.

Jonsson, P., Gullberg, J., Nordstrom, A., Kusano, M., Kowalczyk, M., Sjostrom, M., Moritz, T., 2004. A strategy for identifying differences in large series of metabolomic samples analyzed by GC/MS. Anal. Chem. 76 (6), 1738–1745.

Jonsson, P., Johansson, A.I., Gullberg, J., Trygg, J., A, J., Grung, B., Marklund, S., Sjostrom, M., Antti, H., Moritz, T., 2005. High-throughput data analysis for detecting and identifying differences between samples in GC/MS-based metabolomic analyses. Anal. Chem. 77 (17), 5635–5642.

Khan, W.A., Blobe, G.C., Hannun, Y.A., 1995. Arachidonic acid and free fatty acids as second messengers and the role of protein kinase C. Cell. Signal. 7 (3), 171–184.

Kim, B.O., Liu, Y., Ruan, Y., Xu, Z.C., Schantz, L., He, J.J., 2003. Neuropathologies in transgenic mice expressing human immunodeficiency virus type 1 Tat protein under the regulation of the astrocyte-specific glial fibrillary acidic protein promoter and doxycycline. Am. J. Pathol. 162 (5), 1693–1707.

Larsson, M., Hagberg, L., Norkrans, G., Forsman, A., 1989. Indole amine deficiency in blood and cerebrospinal fluid from patients with human immunodeficiency virus infection. J. Neurosci. Res. 23 (4), 441–446.

Li, W., Galey, D., Mattson, M.P., Nath, A., 2005. Molecular and cellular mechanisms of neuronal cell death in HIV dementia. Neurotox. Res. 8 (1–2), 119–134.

Mahadevan, S., Shah, S.L., Marrie, T.J., Slupsky, C.M., 2008. Analysis of metabolomic data using support vector machines. Anal. Chem. 80 (19), 7562–7570.

Marchio, S., Alfano, M., Primo, L., Gramaglia, D., Butini, L., Gennero, L., De Vivo, E., Arap, W., Giacca, M., Pasqualini, R., Bussolino, F., 2005. Cell surface-associated Tat modulates HIV-1 infection and spreading through a specific interaction with gp120 viral envelope protein. Blood 105 (7), 2802–2811.

Mischiati, C., Pironi, F., Milani, D., Giacca, M., Mirandola, P., Capitani, S., Zauli, G., 1999. Extracellular HIV-1 Tat protein differentially activates the JNK and ERK/MAPK pathways in CD4 T cells. AIDS 13 (13), 1637–1645.

Murray, M.F., 2003. Tryptophan depletion and HIV infection: a metabolic link to pathogenesis. Lancet Infect. Dis. 3 (10), 644–652.

Pasikanti, K.K., Esuvaranathan, K., Ho, P.C., Mahendran, R., Kamaraj, R., Wu, Q.H., Chiong, E., Chan, E.C.Y., 2010. Noninvasive urinary metabonomic diagnosis of human bladder cancer. J. Proteome Res. 9 (6), 2988–2995.

Pendyala, G., Trauger, S.A., Siuzdak, G., Fox, H.S., 2010. Quantitative plasma proteomic profiling identifies the vitamin E binding protein afamin as a potential pathogenic factor in SIV induced CNS disease. J. Proteome Res. 9 (1), 352–358.

Perez, A., Probert, A.W., Wang, K.K., Sharmeen, L., 2001. Evaluation of HIV-1 Tat induced neurotoxicity in rat cortical cell culture. J. Neurovirol. 7 (1), 1–10.

Perry, S.W., Barbieri, J., Tong, N., Polesskaya, O., Pudasaini, S., Stout, A., Lu, R., Kiebala, M., Maggirwar, S.B., Gelbard, H.A., 2010. Human immunodeficiency virus-1 Tat activates calpain proteases via the ryanodine receptor to enhance surface dopamine transporter levels and increase transporter-specific uptake and Vmax. J. Neurosci. 30 (42), 14153–14164.

Petsch, D., Anspach, F.B., 2000. Endotoxin removal from protein solutions. J. Biotechnol. 76 (2–3), 97–119.

Pocernich, C.B., Sultana, R., Mohmmad-Abdul, H., Nath, A., Butterfield, D.A., 2005. HIV-dementia, Tat-induced oxidative stress, and antioxidant therapeutic considerations. Brain Res. Brain Res. Rev. 50 (1), 14–26.

Prakash, O., Teng, S., Ali, M., Zhu, X.Z., Coleman, R., Dabdoub, R.A., Chambers, R., Aw, T.Y., Flores, S.C., Joshi, B.H., 1997. The human immunodeficiency virus type 1 Tat protein potentiates zidovudine-induced cellular toxicity in transgenic mice. Arch. Biochem. Biophys. 343 (2), 173–180.

Prasada Rao, P.V., Gardner, D.E., 1986. Effects of cadmium inhalation on mitochondrial enzymes in rat tissues. J. Toxicol. Environ. Health 17 (2–3), 191–199.

Ramonet, D., Rodriguez, M.J., Fredriksson, K., Bernal, F., Mahy, N., 2004. In vivo neuroprotective adaptation of the glutamate/glutamine cycle to neuronal death. Hippocampus 14 (5), 586–594.

Ruddick, J.P., Evans, A.K., Nutt, D.J., Lightman, S.L., Rook, G.A., Lowry, C.A., 2006. Tryptophan metabolism in the central nervous system: medical implications. Expert. Rev. Mol. Med. 8 (20), 1–27.

Rusnati, M., Presta, M., 2002. HIV-1 Tat protein and endothelium: from protein/cell interaction to AIDS-associated pathologies. Angiogenesis 5 (3), 141–151.

Sabatier, J.M., Vives, E., Mabrouk, K., Benjouad, A., Rochat, H., Duval, A., Hue, B., Bahraoui, E., 1991. Evidence for neurotoxic activity of tat from human immunodeficiency virus type 1. J. Virol. 65 (2), 961–967.

Sabatine, M.S., Liu, E., Morrow, D.A., Heller, E., McCarroll, R., Wiegand, R., Berriz, G.F., Roth, F.P., Gerszten, R.E., 2005. Metabolomic identification of novel biomarkers of myocardial ischemia. Circulation 112 (25), 3868–3875.

Samikkannu, T., Rao, K.V., Gandhi, N., Saxena, S.K., Nair, M.P., 2010. Human immunodeficiency virus type 1 clade B and C Tat differentially induce indoleamine 2,3-dioxygenase and serotonin in immature dendritic cells: implications for neuroAIDS. J. Neurovirol. 16 (4), 255–263.

Schousboe, A., 2003. Role of astrocytes in the maintenance and modulation of glutamatergic and GABAergic neurotransmission. Neurochem. Res. 28 (2), 347–352.

Sekhar, R.V., Jahoor, F., White, A.C., Pownall, H.J., Visnegarwala, F., Rodriguez-Barradas, M.C., Sharma, M., Reeds, P.J., Balasubramanyam, A., 2002. Metabolic basis of HIV–lipodystrophy syndrome. Am. J. Physiol. Endocrinol. Metab. 283 (2), E332–E337.

Shrivastav, S., Kino, T., Cunningham, T., Ichijo, T., Schubert, U., Heinklein, P., Chrousos, G.P., Kopp, J.B., 2008. Human immunodeficiency virus (HIV)-1 viral protein R suppresses transcriptional activity of peroxisome proliferator-activated receptor gamma and inhibits adipocyte differentiation: implications for HIV-associated lipodystrophy. Mol. Endocrinol. 22 (2), 234–247.

Siddappa, N.B., Venkatramanan, M., Venkatesh, P., Janki, M.V., Jayasuryan, N., Desai, A., Ravi, V., Ranga, U., 2006. Transactivation and signaling functions of Tat are not correlated: biological and immunological characterization of HIV-1 subtype-C Tat protein. Retrovirology 3.

Silvers, J.M., Aksenova, M.V., Aksenov, M.Y., Mactutus, C.F., Booze, R.M., 2007. Neurotoxicity of HIV-1 tat protein: involvement of D1 dopamine receptor. Neurotoxicology 28 (6), 1184–1190.

Slama, L., Le Camus, C., Serfaty, L., Pialoux, G., Capeau, J., Gharakhanian, S., 2009. Metabolic disorders and chronic viral disease: the case of HIV and HCV. Diabetes Metab. 35 (1), 1–11.

Smith, S.M., Pentlicky, S., Klase, Z., Singh, M., Neuveut, C., Lu, C.Y., Reitz Jr., M.S., Yarchoan, R., Marx, P.A., Jeang, K.T., 2003. An in vivo replication-important function in the second coding exon of Tat is constrained against mutation despite cytotoxic T lymphocyte selection. J. Biol. Chem. 278 (45), 44816–44825.

Storey, J.D., 2002. A direct approach to false discovery rates. J. R. Stat. Soc. Ser. B 64, 479–498.

Subramanyam, M., Gutheil, W.G., Bachovchin, W.W., Huber, B.T., 1993. Mechanism of HIV-1 Tat induced inhibition of antigen-specific T cell responsiveness. J. Immunol. 150 (6), 2544–2553.

Tabucchi, A., Carlucci, F., Ramazzotti, E., Re, M.C., Marinello, F., Rubino, M., Pagani, R., 1992. Analysis of purine nucleotides in lymphocytes from healthy subjects and AIDS patients. Biomed. Pharmacother. 46 (1), 25–29.

Tabucchi, A., Carlucci, F., Re, M.C., Furlini, G., Consolmagno, E., Leoncini, R., Pizzichini, M., Marinello, E., Rubino, M., Pagani, R., 1993. The behavior of free purine nucleotides in lymphocytes infected with HIV-1 virus. Biochim. Biophys. Acta 1182 (3), 317–322.

Viscidi, R.P., Mayur, K., Lederman, H.M., Frankel, A.D., 1989. Inhibition of antigen-induced lymphocyte proliferation by Tat protein from HIV-1. Science 246 (4937), 1606–1608.

Want, E.J., Nordstrom, A., Morita, H., Siuzdak, G., 2007. From exogenous to endogenous: the inevitable imprint of mass spectrometry in metabolomics. J. Proteome Res. 6, 459–468.

Werner, E.R., Fuchs, D., Hausen, A., Jaeger, H., Reibnegger, G., Werner-Felmayer, G., Dierich, M.P., Wachter, H., 1988. Tryptophan degradation in patients infected by human immunodeficiency virus. Biol. Chem. Hoppe Seyler 369 (5), 337–340.

Wikoff, W.R., Pendyala, G., Siuzdak, G., Fox, H.S., 2008. Metabolomic analysis of the cerebrospinal fluid reveals changes in phospholipase expression in the CNS of SIV-infected macaques. J. Clin. Invest. 118 (7), 2661–2669.